TECHNISCHE MECHANIK, Band 18, Heft 3, (1998), 209-216
Manuskripteingang: 03. Dezember 1997

Multiplicative Thermo-Viscoplasticity: A Thermodynamic Model and its Finite Element Implementation

S. Reese

Most existing models for viscoplastic material behaviour are either of the so-called Perzyna or of the unified type. In the present paper, a model of the unified or overstress type is proposed which includes the Bingham solid, as well as models without an elastic range, as special cases. The approach is very general in the sense that large elastic and large inelastic deformations as well as large deformation rates are taken into account. Furthermore, full thermo-mechanical coupling is considered. The model is based on a multiplicative decomposition of the deformation gradient in elastic and inelastic parts. Due to the modular structure, the finite element implementation remains relatively simple. Existing algorithms for models of finite elasticity or finite plasticity can be adopted with only minor changes.

1 Introduction

Rate-dependent inelastic material behaviour is exhibited by various kinds of materials. Metals and alloys for instance, exhibit such behaviour for temperatures higher than approximately a third of the absolute melting temperature. Models for such material behaviour include the case when the direction of inelastic strain is determined by the total stress, representing the so-called Perzyna-type model (see Perzyna, 1963). A more recent development is the unified approach; in this case, the direction of inelastic strain is determined by the so-called overstress (see Krempl, 1987, and citations therein). The present model fits into this second framework. In contrast to this and other approaches, however, rate-dependent effects are considered in the elastic as well as in the inelastic range. Such material behaviour can be described by a rheological model consisting of a Maxwell element and a Prandtl-Reuss element in parallel (see e.g. Haupt, 1993, and Figure 1). A similar approach has been used to model the behaviour of rubbery polymers by Lion (1997 a,b). For comparison, the Bingham model, representing perhaps the simplest rheological model for viscoplastic material behaviour, consists of damping and friction elements in parallel connected with a Hooke element in series. Such a model could in general apply if the material behaves primarily elastically before yield, and viscoelastically after yield. In contrast, the current model would be relevant if the material shows viscoelastic behaviour both before and after yield. In this way, a wider range of material behaviour can be described. Of course, experiments may reveal that a model as simple as that proposed here, cannot account for the whole variety of special effects. But due to the fact that we are relatively free in the choice of the non-linear elasticity models and the evolution equations, it is expected that a satisfying correlation with experimental results can be achieved without changing the overall structure of the model. Thus, the thermodynamical framework and the finite element formulation remain the same, even if a fitting to experimentals is carried out.

The present work is concerned primarily with the thermo-viscoplastic material behaviour of metals. But the model is also very useful to describe the inelastic behaviour of polymers, which show a wide range of inelastic phenomena, depending on the temperature range chosen. Setting the yield stress equal to infinity yields as special case a typical model for the viscoelastic material behaviour of polymers in the rubbery state (see Reese & Govindjee, 1996). In order not to restrict the range of applications, the model is based on large elastic and large inelastic deformations. Moreover, full coupling between mechanical and thermal fields is considered. The finite element implementation of a similar model can be found in Keck & Miehe (1997) for isothermal problems. An alternative approach for the non-isothermal case is discussed in Lion (1997 b), who also carried out experiments and determined the material parameters of his model on the basis of these. In the present work, we focus on the formulation of the above model and its finite element implementation.

The paper begins with the formulation of the constitutive model for thermoviscoelastic material behaviour. In particular, this involves obtaining forms for the evolution equations (chapter 2) and Helmholtz

free energy (chapter 3). Next, the finite element solution of the evolution, and linear momentum and energy balance equations is discussed. Finally, in order to characterize the behaviour of the proposed model, a numerical example is presented.

2 Constitutive Equations

In order to derive constitutive equations for materials with thermo-viscoplastic behaviour, we use the entropy inequality in the Clausius-Duhem form

$$-\dot{\Psi} + \mathbf{S} : \frac{1}{2}\dot{\mathbf{C}} - s\dot{\Theta} - \frac{1}{\Theta}\mathbf{Q} \cdot \mathrm{Grad}\,\Theta \geq 0 \tag{1}$$

Here, Ψ denotes the Helmholtz free energy per unit reference volume, $\mathbf{S}$ the second Piola-Kirchhoff stress tensor and s the entropy per unit reference volume. For the referential heat flux $\mathbf{Q}$ we have the relationship $\mathbf{Q} = J\,\mathbf{F}^{-1} \cdot \mathbf{q}$, where $\mathbf{q}$ is the spatial heat flux, $\mathbf{F}$ the material deformation gradient and $J = \det \mathbf{F}$. It is assumed further that the constitutively dependent variables Ψ, $\mathbf{S}$, s and $\mathbf{Q}$ are functions of the right Cauchy-Green tensor $\mathbf{C}$, the absolute temperature Θ and n internal variables $(\mathbf{X}_k, k = 1, 2, ..., n)$ to be specified in the following. The heat flux $\mathbf{Q}$ depends additionally on the temperature gradient $\mathrm{Grad}\,\Theta$.

The present material model is based on the rheological model depicted in Figure 1, where the two springs have the stiffnesses E_∞ and E_m and the viscosity of the damping element is denoted by η. σ_Y represents the yield stress. If only small deformations are considered, the decomposition of the total strain ε is additive, leading to the relations between ε_{ep}, ε_{ip}, ε_{ev} and ε_{iv} stated in Figure 1. A decomposition of this kind would not be necessary for the Bingham model, where the strains in the friction and damping elements are equal. As already mentioned above, another difference between the two models is the fact that in the proposed model, the damping element is active from the beginning, i.e. , the material behaviour is rate-dependent both before and after yielding. In the limit of extremely slow loading, both models reduce to the usual Prandtl-Reuss element.

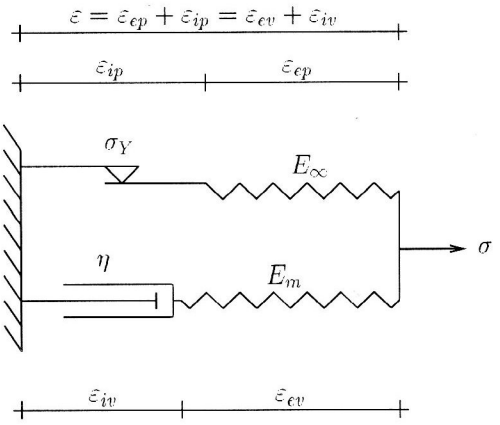

Figure 1. Rheological Model for Viscoplastic Material Behaviour.

Referring to the model depicted in Figure 1, the Helmholtz free energy takes the form

$$\Psi = \underbrace{\frac{1}{2}E_\infty\,(\varepsilon - \varepsilon_{ip})^2}_{\Psi_{pr}} + \underbrace{\frac{1}{2}E_m\,(\varepsilon - \varepsilon_{iv})^2}_{\Psi_m} \tag{2}$$

where Ψ_{pr} (pr stands for Prandtl-Reuss) represents the strain energy in the Prandtl-Reuss spring, whereas Ψ_m is the strain energy in the Maxwell spring. If large deformations and temperature changes are considered, this last form for the free energy can be generalized to that

$$\Psi = \hat{\Psi}_{pr}\,(\mathbf{F}_{ip}^{-T} \cdot \mathbf{C} \cdot \mathbf{F}_{ip}^{-1}, \Theta) + \hat{\Psi}_m\,(\mathbf{F}_{iv}^{-T} \cdot \mathbf{C} \cdot \mathbf{F}_{iv}^{-1}, \Theta) \tag{3}$$

where the multiplicative decompositions

$$\mathbf{F} = \mathbf{F}_{ep} \cdot \mathbf{F}_{ip} = \mathbf{F}_{ev} \cdot \mathbf{F}_{iv} \tag{4}$$

have been applied. Alternatively, $\mathbf{F}_{ip}$ and $\mathbf{F}_{iv}$ could be interpreted as elastic material isomorphisms (see Bertram, 1993, Svendsen, 1997). In the case of isotropic material behaviour, the representation (3) reduces to

$$\Psi = \hat{\Psi}_{pr}\left(\mathbf{b}_{ep}, \Theta\right) + \hat{\Psi}_{pr}\left(\mathbf{b}_{ev}, \Theta\right) \tag{5}$$

where the "elastic" left Cauchy-Green tensors $\mathbf{b}_{ep} = \mathbf{F}_{ep} \cdot \mathbf{F}_{ep}^T = \mathbf{F} \cdot \mathbf{C}_{ip}^{-1} \cdot \mathbf{F}^T$ and $\mathbf{b}_{ev} = \mathbf{F}_{ev} \cdot \mathbf{F}_{ev}^T = \mathbf{F} \cdot \mathbf{C}_{iv}^{-1} \cdot \mathbf{F}^T$ have been introduced. The tensors $\mathbf{C}_{ip}^{-1}$ and $\mathbf{C}_{iv}^{-1}$ function as internal variables $\mathbf{X}_1$ and $\mathbf{X}_2$, respectively. The internal variable $\mathbf{C}_{ip}^{-1}$ is assigned to the rate-independent part of the model. The associated evolution equation

$$\frac{d}{dt}\,\mathbf{C}_{ip}^{-1} = \mathbf{f}_1\left(\mathbf{C}, \dot{\mathbf{C}}, \mathbf{C}_{ip}^{-1}, \Theta, \dot{\Theta}\right) \tag{6}$$

is then required to be a homogeneous function of first order in $\dot{\mathbf{C}}$ and $\dot{\Theta}$. Note that the evolution equations are constructed in such a way that one internal variable does not influence the evolution of the other. This assumption is motivated by the special choice of the rheological model shown in Figure 1. The second internal variable is linked to the rate-dependent part of the model. As such, its evolution is described by a function of $\mathbf{C}$, $\mathbf{C}_{iv}^{-1}$ and Θ:

$$\frac{d}{dt}\,\mathbf{C}_{iv}^{-1} = \mathbf{f}_2\left(\mathbf{C}, \mathbf{C}_{iv}^{-1}, \Theta\right) \tag{7}$$

Inserting the material functions for Ψ, $\mathbf{S}$, s and $\mathbf{Q}$ and the evolution equations in the Clausius-Duhem inequality (1) gives

$$(\mathbf{S} - 2\,\frac{\partial \Psi}{\partial \mathbf{C}}) : \frac{1}{2}\,\dot{\mathbf{C}} - \frac{\partial \Psi}{\partial \mathbf{C}_{ip}^{-1}} : \frac{d}{dt}\,\mathbf{C}_{ip}^{-1} - \frac{\partial \Psi}{\partial \mathbf{C}_{iv}^{-1}} : \frac{d}{dt}\,\mathbf{C}_{iv}^{-1} - (\frac{\partial \Psi}{\partial \Theta} + s)\,\dot{\Theta} - \frac{1}{\Theta}\,\mathbf{Q} \cdot \operatorname{Grad}\Theta \geq 0 \tag{8}$$

The inequality is sufficiently fulfilled, if the constitutive equations

$$\mathbf{S} = 2\,\frac{\partial \Psi}{\partial \mathbf{C}}, \quad s = -\frac{\partial \Psi}{\partial \Theta} \tag{9}$$

and the residual inequality

$$-\frac{\partial \Psi}{\partial \mathbf{C}_{ip}^{-1}} : \frac{d}{dt}\,\mathbf{C}_{ip}^{-1} - \frac{\partial \Psi}{\partial \mathbf{C}_{iv}^{-1}} : \frac{d}{dt}\,\mathbf{C}_{iv}^{-1} - \frac{1}{\Theta}\,\mathbf{Q} \cdot \operatorname{Grad}\Theta \geq 0 \tag{10}$$

are hold. In order to render the last term in (10) non-negative, Fourier's law $\mathbf{q} = -k \operatorname{grad}\Theta$ (k heat conductivity) is assumed. The first two terms are rewritten in the form

$$-\boldsymbol{\tau}_{pr} : \frac{1}{2}\left(\mathcal{L}_v\,\mathbf{b}_{ep}\right) \cdot \mathbf{b}_{ep}^{-1} - \boldsymbol{\tau}_m : \frac{1}{2}\left(\mathcal{L}_v\,\mathbf{b}_{ev}\right) \cdot \mathbf{b}_{ev}^{-1} \geq 0 \tag{11}$$

where the Kirchhoff stress tensor $\boldsymbol{\tau}$ has been split into the Prandtl-Reuss part $\boldsymbol{\tau}_{pr} = 2\,\mathbf{F} \cdot \frac{\partial \Psi_{pr}}{\partial \mathbf{C}} \cdot \mathbf{F}^T$ and the Maxwell part $\boldsymbol{\tau}_m = 2\,\mathbf{F} \cdot \frac{\partial \Psi_m}{\partial \mathbf{C}} \cdot \mathbf{F}^T$. Note that $\boldsymbol{\tau}_{pr}$ also appears in Simo & Miehe (1992), whereas the second term has already been discussed in the context of finite viscoelasticity (see Reese & Govindjee, 1996). The form of the inequality (11), in conjunction with the purely elastoplastic and viscoelastic cases, suggests the forms

$$-\frac{1}{2}\left(\mathcal{L}_v \mathbf{b}_{ep}\right) \cdot \mathbf{b}_{ep}^{-1} = \dot{\gamma}\,\frac{\partial \Phi_{\text{pla}}}{\partial \boldsymbol{\tau}_{pr}} \tag{12}$$

$$-\frac{1}{2}\left(\mathcal{L}_v \mathbf{b}_{ev}\right) \cdot \mathbf{b}_{ev}^{-1} = \frac{1}{\tau}\,\frac{\partial \Phi_{\text{vis}}}{\partial \boldsymbol{\tau}_m} \tag{13}$$

for the evolution relations, where the plastic potential Φ_{pla} represents the yield function, and the so-called viscoelastic potential $\Phi_{\text{vis}} = \frac{\tau}{2}\boldsymbol{\tau}_m : \mathcal{V}^{-1} : \boldsymbol{\tau}_m$ is defined by means of the fourth order tensor $\mathcal{V}^{-1}$ given by

$$\mathcal{V}^{-1} = \frac{1}{2\underbrace{\hat{\mu}_m(\Theta)\,\hat{\tau}(\mathbf{b}_{ev},\Theta)}_{\eta_D}}(\mathbf{1}^4 - \frac{1}{3}\mathbf{1}\otimes\mathbf{1}) + \frac{1}{9\underbrace{\hat{K}_m(\Theta)\,\hat{\tau}(\mathbf{b}_{ev},\Theta)}_{\eta_V}}\mathbf{1}\otimes\mathbf{1} \tag{14}$$

This so-called inverse viscosity tensor $\mathcal{V}^{-1}$ is constructed in such a way that in the limit of small deformation rates, or in other words, if only small perturbations away from thermodynamic equilibrium are considered, the linear evolution equation

$$\frac{1}{2}(\mathcal{L}_v\mathbf{b}_{ev})\cdot\mathbf{b}_{ev}^{-1} = \frac{1}{2\tau}(\mathbf{b}_{ev} - \mathbf{1}) \tag{15}$$

is recovered. In the context of the finite element implementation, the analogous forms of (12) and (13) will be very useful, as shown below.

3 Helmholtz Free Energy

In the derivation of the constitutive relations for $\mathbf{S}$ and s and the evolution equations (12) and (13), the temperature dependence could be included without complicating the analysis. This, however, is not the case for the Helmholtz free energy, which has to be formulated in such a way that the internal energy e and the heat capacity c are thermodynamically consistent. These issues have been discussed in detail by Chadwick (1974). In the paper of Chadwick (1974), one finds the general form for

$$\Psi = \Psi_0\frac{\Theta}{\Theta_0} + e_0(1 - \frac{\Theta}{\Theta_0}) + \int_{\Theta_0}^{\Theta} c\,(1 - \frac{\Theta}{\widetilde{\Theta}})\,d\widetilde{\Theta} \tag{16}$$

where the heat capacity c is given by

$$c = -\Theta\frac{\partial^2\Psi}{\partial\Theta^2} = c_\infty + c_m \tag{17}$$

and e_0 denotes the internal energy $e = \Psi + \Theta s$ evaluated at the reference temperature Θ_0. If the heat capacity is assumed to be constant ($c = \bar{c}$), the stresses are at the most linear functions of the temperature. Experimental observations, however, show that such a linear relation is not always realistic. In order to work with a non-linear relation, we introduce the function $\hat{g}(\Theta)$. Using

$$c = \bar{c} - \Theta\frac{\partial^2 g}{\partial\Theta^2}\Psi_0 \tag{18}$$

the Helmholtz free energy can be expressed by

$$\Psi = e_0(1 - \frac{\Theta}{\Theta_0}) + \bar{c}\,(\Theta - \Theta_0 - \Theta\ln\frac{\Theta}{\Theta_0}) + \left(\frac{\Theta}{\Theta_0} + \hat{g}(\Theta) - \hat{g}(\Theta_0) + \left.\frac{\partial g}{\partial\Theta}\right|_{\Theta_0}(\Theta_0 - \Theta)\right)\Psi_0 \tag{19}$$

It is evident that a non-linear dependence of the stresses on the temperature can now be taken into account. Note that g could, for example, take the form $g = b\,(\frac{\Theta}{\Theta_0})^a$, with the material parameters a and b determined by means of experiments. Special cases of (19) are

$$\Psi = (\Psi_0)_{pr} + \alpha_T\,\hat{f}(J_{ep}) \quad\text{and}\quad \Psi = \frac{\Theta}{\Theta_0}((\Psi_0)_\infty + (\Psi_0)_m) + \alpha_T\,\hat{f}(J) \tag{20}$$

Here, J_{ep} denotes the determinant of $\mathbf{F}_{ep}$ and α_T represents the thermal expansion coefficient. Whereas the first form is rather appropriate to model the elasto-plastic material behaviour of steel, the latter is typical for the so-called purely entropic viscoelastic behaviour of rubber. In contrast to steel, where viscous effects are often neglected, rubber exhibits clearly rate-dependent material behaviour while the plastic deformation being of subordinate importance. In this way, the form (19) allows to describe a

wide range of material behaviour. The choice of a special model is only controlled by the imput file which makes the present approach very useful in practical applications.

4 Numerical Issues

In this section, two aspects of the numerical treatment of the constitutive model described in the above are discussed. The first concerns the solution of the evolution equations (12) and (13). In the second part, the weak forms of the balance of linear momentum and the balance of energy are given and discussed from the numerical point of view. It is important to note that the integration of the evolution equations is carried out on local level, i.e. in the Gauss point in a finite element context. The solution of the weak forms, however, cannot be done before the finite element vectors and matrices have been assembled. Neglecting the inertia terms, this requires the time integration of the energy balance.

Since the evolution equations (12) and (13) have an analogous structure, the time integration of these equations can be carried out in the same way. Efficient algorithms for that can be found in the literature, usually in relation with isothermal elastoplasticity (see e. g. Weber & Anand, 1990, and Eterovic & Bathe, 1990). Caused by the fact that the evolutions of the internal variables $\mathbf{C}_{ip}^{-1}$ and $\mathbf{C}_{iv}^{-1}$ are completely decoupled from each other, we can treat each evolution process seperately. Furthermore, the temperature plays the same role as the so-called "trial" strain, i.e. , both quantities are so-called global variables. As such, they are held constant on local level. Taking this into account allows us to proceed here as in the isothermal case. The only important difference between the plastic and the viscous part lies in the fact that the plastic part requires to consider the side condition $\Phi_{\text{pla}} \leq 0$. Thus, for the local integration of the present constitutive model, it suffices to combine already existing and validated algorithms. This makes the implementation of the model very simple, especially if such algorithms have already been used within another program. For more details in finite viscoelasticity see Reese & Govindjee (1996).

In the present initial boundary value problem, the balance of linear momentum and the balance of energy are solved in weak form, whereas the balances of mass and angular momentum are satisfied due to $\rho = \rho_0 J$ and $\boldsymbol{\tau} = \boldsymbol{\tau}^T$, respectively. The weak form of linear momentum takes the form

$$\int_{\mathcal{B}_0^h} \frac{1}{2}\boldsymbol{\tau}^h : (\mathbf{F}^{-T} \cdot \delta\mathbf{C} \cdot \mathbf{F}^{-1})^h \, dV^h - \int_{\partial\mathcal{B}_{0P}^h} \bar{\mathbf{T}} \cdot \delta\mathbf{u}^h \, dA^h = 0 \tag{21}$$

where the volumetric force and the inertia force have been neglected. $\delta\mathbf{C}$ is defined by $\delta\mathbf{C} = \text{sym}\,(\delta\mathbf{F}^T \cdot \mathbf{F})$. On the boundary $\partial\mathcal{B}_{0u}^h$, the displacement vector is given by $\mathbf{u} = \bar{\mathbf{u}}$, whereas on the boundary $\partial\mathcal{B}_{0P}^h$, tractions (stress vector $\mathbf{T} = \bar{\mathbf{T}}$) are prescribed. The index h indicates that we deal here with the discrete form of the variational formulation. In the present finite element formulation, linear approximations for $\mathbf{u}$ and Θ are chosen.

The thermomechanical coupling in this balance equation is contained in the temperature dependence of the Kirchhoff stress tensor $\boldsymbol{\tau} = \hat{\boldsymbol{\tau}}\,(\mathbf{b}_{ep}, \mathbf{b}_{ev}, \Theta)$, which leads to a temperature-dependence of the deformation. In particular, the coupling effect is due to the deformation resulting from thermal expansion (controlled by the thermal expansion coefficient α_T), as well as the temperature-dependence of the material parameters, in particular that of the relaxation time, the yield stress and the hardening modulus.

The balance of energy in weak form is given by

$$\int_{\mathcal{B}_0^h} J^h \, \mathbf{q}^h \cdot \text{grad}\,\delta\Theta^h \, dV^h + \int_{\mathcal{B}_0^h} (-w_{\text{int}}^h + w_{\text{ext}}^h - c^h \dot{\Theta}^h)\,\delta\Theta^h \, dV - \int_{\partial\mathcal{B}_{0Q}^h} \bar{Q}\,\delta\Theta \, dA^h = 0 \tag{22}$$

where the quantities w_{int} and w_{ext} are defined by

$$w_{\text{int}} = (\boldsymbol{\tau}_m - \Theta \frac{\partial\boldsymbol{\tau}_m}{\partial\Theta}) : \frac{1}{2}\mathcal{L}_v\mathbf{b}_{ev} \cdot \mathbf{b}_{ev}^{-1} + (\boldsymbol{\tau}_{pr} - \Theta \frac{\partial\boldsymbol{\tau}_{pr}}{\partial\Theta}) : \frac{1}{2}\mathcal{L}_v\mathbf{b}_{ep} \cdot \mathbf{b}_{ep}^{-1} = \hat{w}_{\text{int}}\,(\mathbf{b}_{ev}, \mathbf{b}_{ep}, \Theta) \tag{23}$$

and

$$w_{\text{ext}} = \Theta\,(\frac{\partial\boldsymbol{\tau}_{pr}}{\partial\Theta} + \frac{\partial\boldsymbol{\tau}_m}{\partial\Theta}) : \mathbf{d} = \hat{w}_{\text{ext}}\,(\mathbf{b}_{ep}, \mathbf{b}_{ev}, \Theta, \mathbf{d}) \tag{24}$$

For simplicity, the index h has been dropped in the latter two equations. Note that $\mathbf{d}$ represents the symmetric part of the spatial velocity gradient $\mathbf{l} = \operatorname{grad} \mathbf{v}$. On the boundary $\partial\mathcal{B}^h_{0\Theta}$ the temperature is known, whereas the heat flux ($\bar{Q} = \bar{\mathbf{Q}} \cdot \mathbf{N}^h$) is prescribed on the boundary $\partial\mathcal{B}^h_{0Q}$. We have further $\partial\mathcal{B}^h_0 = \partial\mathcal{B}^h_{0u} \cup \partial\mathcal{B}^h_{0P} = \partial\mathcal{B}^h_{0\Theta} \cup \partial\mathcal{B}^h_{0Q}$ ($\partial\mathcal{B}^h_{0u} \cap \partial\mathcal{B}^h_{0P} = \emptyset, \partial\mathcal{B}^h_{0\Theta} \cap \partial\mathcal{B}^h_{0Q} = \emptyset$). Finally, initial conditions have to be defined: $\mathbf{u}^h(\mathbf{X}, t=0) = \mathbf{0}$, $\hat{\Theta}^h(\mathbf{X}, t=0) = \Theta_0$.

The two terms, w_{int} and w_{ext}, describe the dissipation of mechanical energy into heat. The size of the latter contribution, however, is mainly controlled by the velocity field, whereas the first is in particular influenced by the evolution of the internal variables. For this reason, we have chosen here the notions internal and external dissipation of energy. Furthermore, it is worth emphasizing, that the internal dissipation term is only present in the case of an inelastic problem, whereas the external dissipation of energy takes place even in a thermoelastic problem.

The weak forms are solved by using Newton's method which requires a consistent linearization of the two equations. Note that the tangent operator is not symmetric which is due to the thermo-mechanical coupling. The mechanical part of the model alone would provide still a symmetric tangent, since both evolution equations are based on a potential. As element formulation, we use here the standard isoparametric displacement formulation. For the present example this element performs sufficiently well. Note, however, that in bending situations or nearly incompressible problems, in order to avoid locking, the use of mixed formulations is recommended.

5 Example

As example, we investigate the compression of a steel block. The geometry and the loading of the structure are depicted in Figure 2. The boundary conditions are chosen in such a way that the top of the structure is constrained in the horizontal and vertical direction. At the bottom, the block is allowed to move in horizontal direction, except at the middle node, which is held fixed. As for the temperature, it is prescribed at the top of the structure, and otherwise allowed to develop freely. On the other boundaries, the heat flux is set to zero.

The following material parameters are used:

$$\begin{gathered} \mu_\infty = 80769\,\mathrm{N/mm^2};\quad K_\infty = 121154\,\mathrm{N/mm^2} \\ \mu_m = \mu_\infty/2;\quad K_m = K_\infty/2;\quad \tau = 1\,\mathrm{s} \\ \sigma_Y = 450\,\mathrm{N/mm^2};\quad H = 129\,\mathrm{N/mm^2};\quad \omega_Y = 0.002;\quad \omega_H = 0.002 \\ \alpha_T = 1.2 \cdot 10^{-5}\,1/\mathrm{K};\quad k = 45\,\mathrm{N/(K\,s)};\quad \bar{c} = 3.768\,\mathrm{N/(mm^2\,K)} \end{gathered} \tag{25}$$

The elastic material behaviour in the Prandtl-Reuss element as well as in the Maxwell element is modeled by means of a compressible Neo-Hooke model. The temperature dependence of the yield stress σ_Y and the hardening modulus H is controlled by the two parameters ω_Y and ω_H, respectively. The heat capacity is held constant.

If the block is compressed extremely slowly, the material behaves approximately thermo-plastically. The heating of the structure and the distribution of the temperature is shown in Figure 3. Due to having no heat exchange with the surroundings on three of the four boundaries, as well as the dissipative generation of heat internally, the temperature increases noticeably. In particular, due to $\mathbf{d} \approx \mathbf{0}$, the heat generation is here caused by the energy dissipation term w_{int}. This being the case, the distribution of the plastic equivalent strain and the distribution of the temperature are very similar. This is, however, not the case before the yield stress is reached, since then only the external energy dissipation is present, which is negligible for very low loading velocities (see Figure 4.)

In Figure 5, the temperature distribution for the same total load, but different loading velocities, is plotted. Here, we see that, the faster the loading, the smaller the temperature increase. In addition, the structure then behaves more stiffly. Indeed, for very slow loading, the stress in the Maxwell element is negligible. In this case, the deformation of the structure is controlled solely by the Prandtl-Reuss element. For a higher loading velocity, however, the Maxwell part of the model also contributes to the stress state in the structure. Consequently, this increases the stiffness.

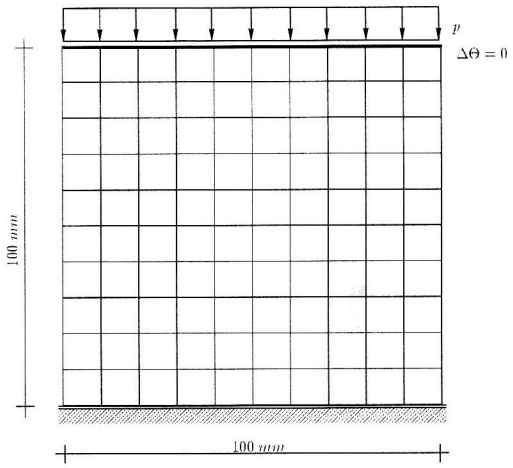

Figure 2. Steel Block under Compression.

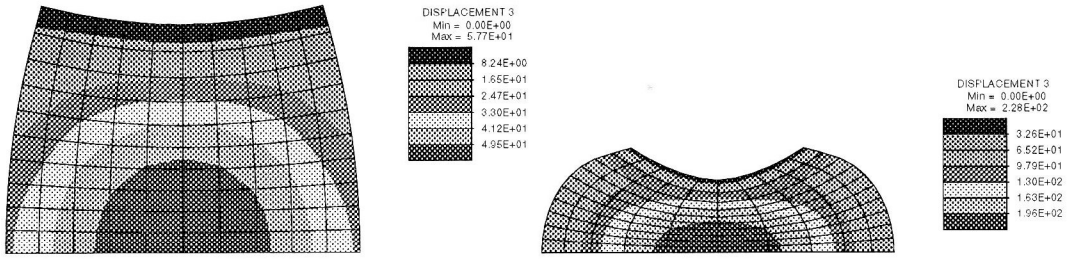

Figure 3. Temperature Distribution for Two Different Compression States: (a) $\Delta\Theta_{\max} = 57.1\,\mathrm{K}$, (b) $\Delta\Theta_{\max} = 228\,\mathrm{K}$

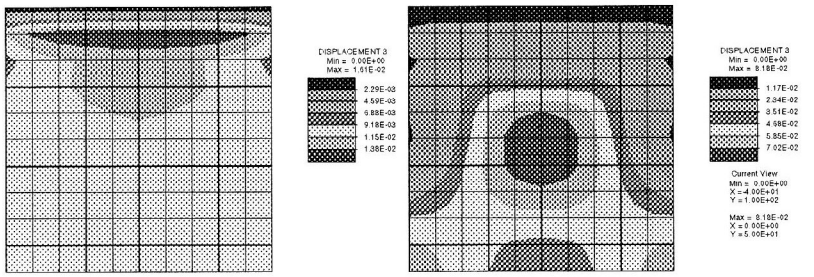

Figure 4. Temperature Distribution: (a) Before Yield ($\Delta\Theta_{\max} = 0.0151\,\mathrm{K}$), (b) After Partial Yield ($\Delta\Theta_{\max} = 0.0818\,\mathrm{K}$).

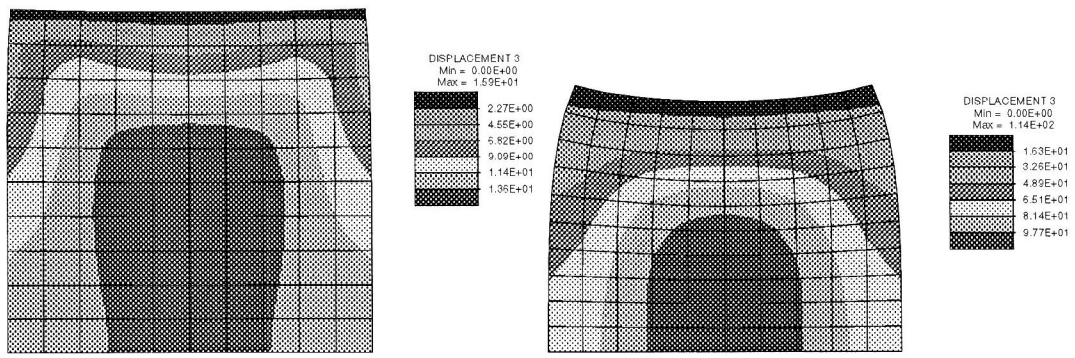

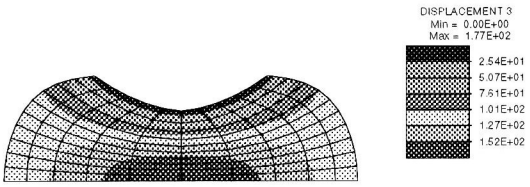

Figure 5. Temperature distribution: (a) $\dot{F} = 30\,\mathrm{kN/s}$ ($\Delta\Theta_{\max} = 15.9\,\mathrm{K}$), (b) $\dot{F} = 3\,\mathrm{kN/s}$ ($\Delta\Theta_{\max} = 114\,\mathrm{K}$), (c) $\dot{F} = 0.3\,\mathrm{kN/s}$ ($\Delta\Theta_{\max} = 177\,\mathrm{K}$)

6 Conclusions

Considering the fact that large elastic and large inelastic deformations as well as full thermo-mechanical coupling are taken into account, the computational effort is astonishingly small. What remains is a comparison with experimental results which will be pursued in a future work, based on data published in earlier literature.

Literature

1. Bertram, A.: Description of Finite Elastic Deformations, in: MECAMAT '92, "Multiaxial Plasticity", A. Benallal, R. Billardon & D. Marquis, ed., (1993), 821–835.
2. Chadwick, P.: Thermomechanics of Rubberlike Materials, Trans. Royal Soc. London (A 276), (1974), 371–403.
3. Eterovic, A. L., Bathe, K.-J.: A Hyperelastic-Based Large Strain Elastoplastic Constitutive Formulation with Combined Isotropic-Kinematic Hardening Using the Logarithmic Stress and Strain Measures, Int. J. Num. Eng. 30, (1990), 1099–1114.
4. Haupt, P.: On the Mathematical Modelling of Material Behaviour in Continuum Mechanics, Acta Mechanica 100, (1993), 129–154.
5. Keck, J., Miehe, C.: An Eulerian Overstress-Type Viscoplastic Constitutive Model in Spectral Form. Formulation and Numerical Implementation, in: "Computational Plasticity, Fundamentals and Applications", D. R. J. Owen, E. Onate & E. Hinton, ed., (1997), 996–1003.
6. Krempl, E.: Models of Viscoplasticity – Some Comments on Equilibrium (Back) Stress and Drag Stress, Acta Mechanica 69, (1997), 25–42.
7. Lion, A.: On the Mathematical Representation of the Thermomechanical Behaviour of Elastomers, Acta Mechanica 123, (1997), 1–25.
8. Lion, A.: On the Large Deformation Behaviour of Reinforced Rubber at Different Temperatures, J. Mech. Phys. Sol. 45, (1997), 1805–1834.
9. Perzyna, P.: The Constitutive Equations for Rate Sensitive Plastic Materials, Quarterly Appl. Math. 20, (1963), 321–332.
10. Reese, S., Govindjee, G.: A Theory of Finite Viscoelasticity and Numerical Aspects, to appear in Int. J. Sol. Struct., (1998).
11. Simo, J. C., Miehe, C.: Associative Coupled Thermoplasticity at Finite Strains: Formulation, Numerical Analysis and Implementation, Comp. Meths. Appl. Mech. Eng. 98, (1992), 41–104.
12. Svendsen, B.: A Thermodynamic Formulation of Finite-Deformation Elastoplasticity with Hardening Based on the Concept of Material Isomorphism, to appear in International Journal of Plasticity, (1998).
13. Weber, G., Anand, L.: Finite Deformation. Constitutive Equations and a Time Integration Procedure for Isotropic Hyperelastic-Viscoelastic Solids, Comp. Meths. Appl. Mech. Eng. 79, (1990), 173–202.

Address: Dr.-Ing. Stefanie Reese, Institut für Mechanik (AG IV), Technische Universität Darmstadt, Hochschulstr. 1, D-64289 Darmstadt